Enhancing the test time performance of Ludwieg Tunnels

Jack Hillyer*, Luke Doherty†, Chris Hambidge ‡, and Matthew McGilvray§
University of Oxford

Ground testing at hypersonic conditions requires either expensive heating or reduced test time. This paper discusses further developments to a mode of operation for Ludwieg Tunnels - Plenum Augmented Ludwieg Mode (PALM) - in the Oxford High Density Tunnel (HDT). PALM offers increased test time performance relative to standard Ludwieg Mode at the expense of total pressure and unit Reynolds number capability. A description of the theory of operation and the implementation of PALM in the HDT is given. Experimental results, quasi-1D numerical simulations and a performance map are presented. PALM has been demonstrated to offer a factor of 10 increase in the test time with a reduction in maximum Unit Reynolds number of approximately 50% relative to standard Ludwieg Mode. Theoretical performance maps predict that PALM can offer a factor of 10 improvement in test time for all Mach 7 unit Reynolds numbers run to date in HDT without any facility upgrades. Hence, operation in PALM significantly improves the capability of the HDT to investigate unsteady and long duration flow phenomena relative to standard Ludwieg Mode operation.

Nomenclature

a	=	Speed of sound, m s^{-1}
L	=	Barrel Length, m
p_0	=	Nozzle Supply Pressure, Pa
Re_u	=	Unit Reynolds Number m^{-1}
T_0	=	Total Temperature, K
t_{op}	=	Opening time of the fast acting valve, s
t_{wr}	=	Time taken for the rarefaction wave to return to the valve, s
x_1	=	Plug valve piston displacement for plug valve to be fully open, m
x_{wr}	=	Plug valve piston displacement at t_{wr}, m
ELM	=	Extended Ludwieg Mode
HDT	=	Oxford High Density Tunnel
LM	=	Ludwieg Mode
$PALM$	=	Plenum Augmented Ludwieg Mode

I. Introduction

Extensive ground testing is used during the design of a hypersonic vehicle for two key purposes: 1) as a cheap, low-risk alternative to flight tests for determining vehicle characteristics and behaviour [1] and 2) in support of CFD studies via provision of validation data and investigation of un-modelled phenomena [2–4]. However, the hypersonic flight regime is inherently complex and a single wind tunnel is not capable of replicating all of the effects of hypersonic flight simultaneously. For this reason, ground testing is often performed in an array of hypersonic facilities, each with their own limitations [5]. One limitation common to all hypersonic facilities is their intermittent operation: test times are limited to minutes at most and are typically inversely proportional to flow enthalpy [6]. Enthalpy matched, full scale, continuous hypersonic wind tunnels are not feasible due to high structural and thermal loads and total power required (order of GigaWatts) [7].

For short duration intermittent hypersonic facilities like those typically operated within Universities, the duration

*DPhil Candidate, Department of Engineering Science, jack.hillyer@eng.ox.ac.uk
†Departmental Lecturer, Department of Engineering Science, AIAA member, luke.doherty@eng.ox.ac.uk
‡Hypersonic Facilities Manager, Department of Engineering Science
§Professor, Department of Engineering Science

of the test flow directly influences the experiments that can be performed as it dictates which flow properties have established. The length of test time required for the flow to establish is typically measured in flow lengths - the length of time it takes for a packet of fluid to reach a location of interest on a model - as it inherently accounts for the size of the facility/model. It is well known that pressure requires approximately one flow length to establish, whereas skin friction and heat transfer require up to three flow lengths depending on the state of the boundary layer [8, 9]. Unsteady effects, such as separation and recirculation regions, require significantly longer to establish - for instance recirculation regions on backwards facing steps such as those behind scramjet injectors can take up to 140 flow lengths [10]. These longer establishment times can sometimes be accommodated in short duration facilities by reducing the size of the model, but this comes at the cost of model complexity and a loss of spatial data resolution. An increase in available test time allows for larger models to be used (up to the blockage limit) and could greatly expand the capability of the facility to investigate unsteady phenomena, such as Fluid-Structural-Interaction, unstart of high speed inlets, or investigation of wake flows. However, the benefits of increased test time are not limited to unsteady experiments - force balance measurements are simplified as stress waves internal to the model have sufficient time to equilibrate, allowing manufacturer supplied static calibrations to be used [11–13]. Additionally, longer test times allow for multiple model attitudes to be characterised in a single run, reducing the total number of tests required.

One common type of low enthalpy, short duration hypersonic facility is a Ludwieg Tunnel. These typically produce cold perfect gas flows, capable of simulating flight Mach and Reynolds number but not high temperature gas effects. A Ludwieg Tunnel generally consists of a barrel filled with high pressure gas connected to a nozzle via a fast-acting valve or a diaphragm. Fig. 1a shows a schematic diagram and distance-time (x-t) wave plot for a Ludwieg tunnel operating in Ludwieg Mode (LM). In LM, flow is initiated by rapidly opening a valve or bursting a diaphragm, resulting in a rarefaction wave travelling upstream. Steady supply conditions to the facility nozzle are attained until the rarefaction wave returns to the nozzle throat, resulting in a decrease in supply pressure. Unless the test is then terminated, the rarefaction wave reflects, and the process repeats. This results in a classic Ludwieg trace consisting of several steady flow plateaus, shown schematically in Fig. 1a. The length of each plateau, t_{wr}, is given by the length of time it takes for the rarefaction wave to return to the valve/diaphragm:

$$t_{wr} \approx \frac{2L}{a} \tag{1}$$

Where L is the length of the facility barrel and a is the speed of sound of the gas in the barrel. For the Oxford High Density Tunnel, t_{wr} varies between 35-50 ms [14].

Traditionally, extension of test times in Ludwieg tunnels is achieved via an increase in facility length [15]. Jones [16] proposed two new modes of operation for Ludwieg Tunnels aimed at extending the test time: Extended Ludwieg Mode (ELM) and Plenum Augmented Ludwieg Mode (PALM), x-t and p-t diagrams of which are shown in Fig. 1b and

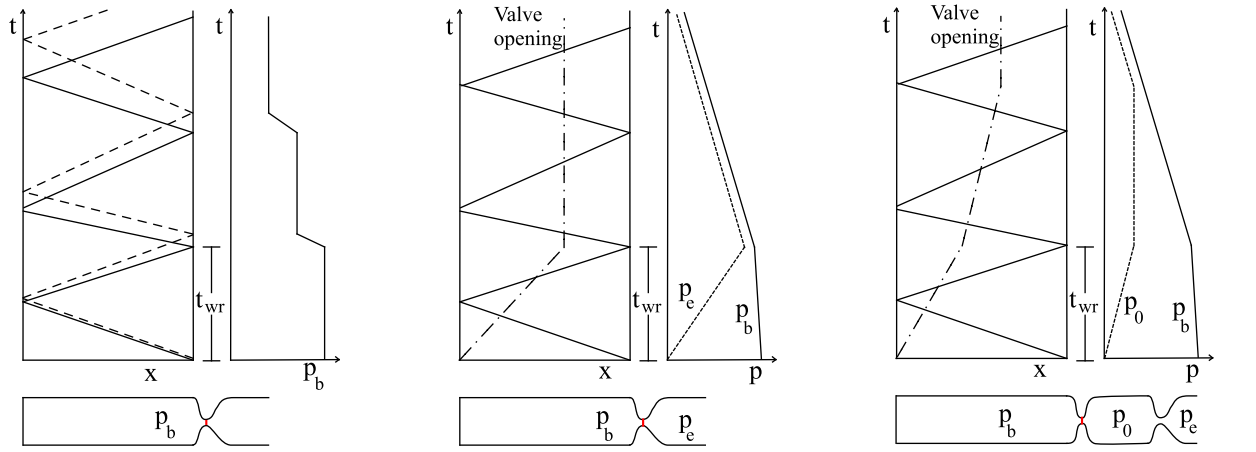

(a) Ludwieg Mode (b) Extended Ludwieg Mode c) Plenum Augmented Ludwieg Mode

Fig. 1 x-t and p-t diagrams of a Ludwieg tunnel operating in Ludwieg Mode, Extended Ludwieg Mode and Plenum Augmented Ludwieg Mode. The red line in the schematic indicates the location of the fast acting valve or diaphragm

Fig. 1c, respectively. In ELM, the opening time of the valve is increased to equal t_{wr}, extending the rarefaction wave and resulting in a steady decrease in nozzle supply pressure(Fig. 1b). This sacrifices the steadiness of a LM plateau, but greatly extends the test duration. PALM requires the Ludwieg Tunnel to have a dual-throat arrangement, with a plenum between the barrel and the facility nozzle and the plug valve located between barrel and plenum rather than at the nozzle throat. The barrel is then operated in ELM and the valve opening is adjusted to balance the head loss across the valve to the decrease in barrel pressure. This results in constant supply pressure to the facility nozzle, greatly extending the available steady test time to be comparable to some blowdown facilities (without an increase in size of the Ludwieg tunnel). However, this extension of test time comes at the expense of total pressure and unit Reynolds number capability. If higher unit Reynolds numbers are required, the tunnel must be operated in Ludwieg Mode. Both ELM and PALM have previously been implemented in the HDT [17], but the duration of the PALM supply pressure trace was limited by the plug valve pipework. ELM is now fully commissioned as an alternative to LM across HDT's current range of operating pressures, but PALM is still under development. This paper discusses the theory of operation of PALM in Section II, and a description of the facility, including new plug valve pipework, is given in Section III. Experimental results are given in Section IV and finally a performance map is presented in Section V.

II. Theory of operation

A detailed explanation of the theory of PALM and the effect of different valve openings on the resultant supply pressure trace is given in [17]. To summarise, operation in PALM requires the Ludwieg Tunnel to have two features: 1) The facility must have a plenum upstream of the nozzle throat and 2) the facility valve must be designed such that the head loss across it is a function of valve opening. If these two conditions are met, the opening of the fast acting valve can be tailored to extend the test time available in the Ludwieg Tunnel.

A schematic x-t wave diagram of a Ludwieg Tunnel operating in PALM, with required valve opening overlaid, is shown in Fig. 2. To achieve PALM operation, the valve opening must feature two distinct stages. The first, occurring between time zero and t_{wr}: *partial opening* of the valve. This partial, slow opening extends the rarefaction wave, resulting in a constant decrease of barrel pressure. The valve opening at the end of this stage governs the supply pressure of the plateau, with greater opening leading to higher supply pressures. The second stage tailors the remaining valve opening to balance the decreases in barrel pressure and head loss to produce a plateau. Fig. 2 shows the steadiness of the plateau is determined by the speed of valve opening in the second stage. If the valve opening is too fast, the supply pressure decreases (Fig. 2b). Conversely, if the valve opening is too slow, the supply pressure increases (Fig. 2c).

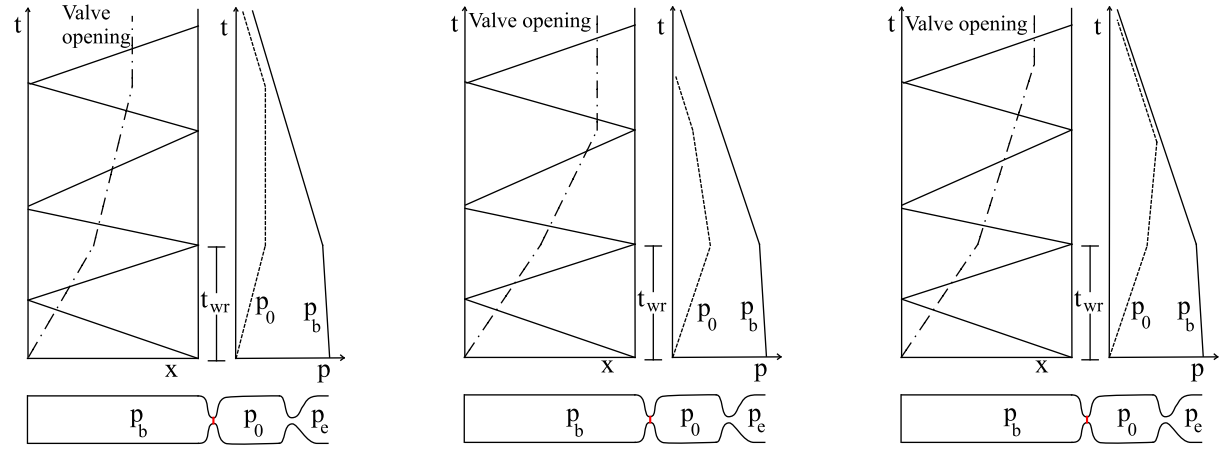

(a) Tailored PALM (b) Second stage motion too fast c) Second stage motion too slow

Fig. 2 Schematic x-t and p-t diagrams showing the effect of different valve openings on the resultant PALM supply pressure trace trace. The red line in the schematics indicates the location of the fast acting valve

III. Oxford High Density Tunnel

The Oxford High Density Tunnel (HDT) is a Ludwieg tunnel located at the Oxford Thermofluids Institute, University of Oxford [18]. A schematic of the facility is given in Fig. 3, featuring a barrel of internal diameter 152 mm and length 17.35 m. The barrel is separated from the nozzle plenum by an upstream facing plug valve. The HDT features four operational nozzles, each with an exit diameter of 351 mm, covering the range of Mach 4 to Mach 7. The facility barrel can be heated to 550 K, and has a maximum pressure rating of 275 bar.

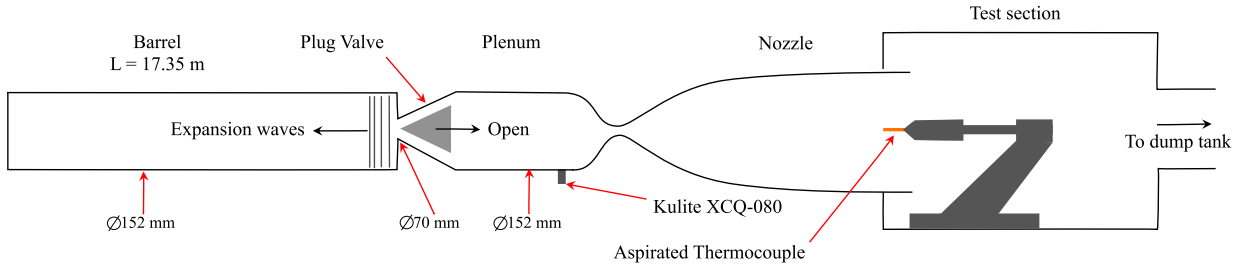

Fig. 3 Schematic of the Oxford High Density Tunnel with a Pitot rake installed. The indicated Kulite and aspirated thermocouple provide measurements of the facility supply pressure and total temperature respectively. Reproduced from [19]

A. Plug valve

HDT features an upstream facing, fast acting plug valve between the facility barrel and plenum. The plug valve is pneumatically actuated, with opening and closing achieved by venting and pressurising the volume behind the piston. A key feature of the HDT plug valve is the slots in the piston housing, exposed as the piston displaces, which provide the head loss variation required for PALM. The maximum area through the gas slots is greater than the area of the plug valve throat, and consequently there are two important piston positions for operation of HDT in PALM:

1) x_1: The exposed area of the gas slots is equal to the area of the plug valve throat
2) x_{wr}: Piston displacement at t_{wr}

When the piston is at x_1, the flow no longer sees a restriction from the piston, and the plug valve can be defined as fully open. If $x_{wr} < x_1$, the barrel pressure will constantly decrease, and PALM can be achieved.

The desired plug valve opening for PALM is achieved by installation of the PALM pipework in the plug valve vent line. The PALM pipework was upgraded for this work and now features three branches, all fitted with different sized orifices. Pilot operated solenoid valves are installed on two of the branches, allowing for 4 different venting flow rates to be achieved.

B. Instrumentation

The facility nozzle supply pressure was measured using a flush mounted Kulite XCQ-080 pressure transducer, and a Pitot rake was used to characterise the test condition. The Pitot pressure was measured at 6 radial locations with Kulite pressure sensors, and the total temperature calculated from aspirated thermocouple data collected at two radial locations using the processing outlined in [19]. The amplifiers used were Fylde FE-H379TA's for the Kulites and Fylde 351UA's for the thermocouples. The thermocouples were recorded at 100kHz, but as these tests were in an experimental mode of operation, the Kulites were recorded for a longer duration at 10kHz to ensure that the full behaviour of the tunnel was captured. Unfortunately, this lower sampling rate precludes a comparison of the freestream noise between LM, ELM, and PALM.

IV. Experimental Results

This section presents experimental results from testing of PALM in the HDT at Mach 7 with fill conditions of 14 bar, 500 K. LM and ELM data is reproduced from [17] to provide context of PALM performance against currently commissioned HDT modes.

Fig 4a shows a comparison of supply pressures attained across the three modes of operation. The LM and ELM traces are as expected, with LM producing several steady flow plateaus and ELM a constant decrease in supply pressure.

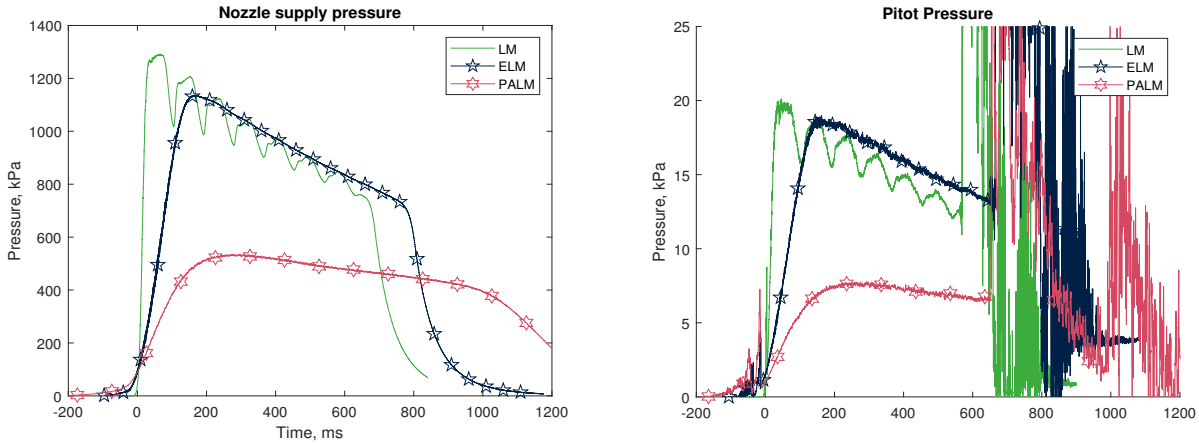

(a) Supply Pressure

(b) Pitot Pressure

Fig. 4 Experimental Pitot and supply traces at Mach 7, 14 bar, 500K fill. All traces have been filtered with a 1 kHz **low pass filter**

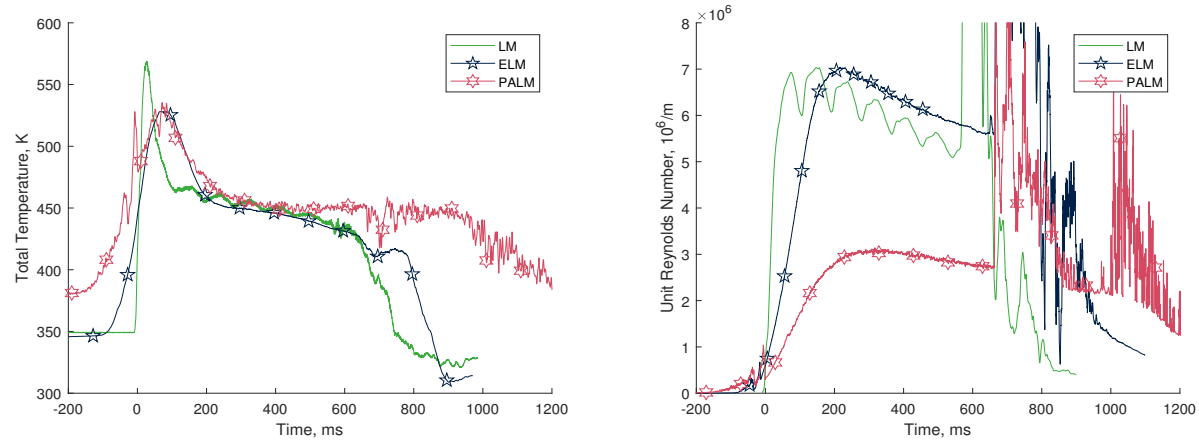

(a) Total Temperature

(b) Unit Reynolds Number

Fig. 5 Experimental total temperature and unit Reynolds number traces at Mach 7, 14 bar, 500K fill

Table 1 Flow steadiness and achieved test time for each mode. All values for LM have been averaged on the second plateau

Mode	$\lvert\frac{dp_0}{dt}\rvert$, kPa s^{-1}	$\lvert\frac{dT_0}{dt}\rvert$ K s^{-1}	$\lvert\frac{dRe_u}{dt}\rvert$, x10^6 s^{-1} m^{-1}	Test Time
LM	859	62.5	6.35	35
ELM	733	58.1	3.49	500
PALM	172	11.2	0.98	400

The PALM trace exhibits a steady decrease in supply pressure, but at a reduced rate relative to ELM. This indicates that the second stage motion of the piston was too fast for ideal PALM operation (see Fig. 2b). Regardless, the PALM trace exhibits a potential test time of 700 ms, a factor of 20 improvement over a Ludwieg Mode plateau, demonstrating that the upgraded PALM pipework has alleviated the previous issue with premature termination of the supply pressure trace [17].

Fig 4b shows a comparison of Pitot pressures across the three modes of operation. In all cases, the Pitot pressure

follows the supply pressure traces as expected. However, facility unstart can be observed in each of the traces, with unstart occurring earliest in the LM case due to having the highest mass flow rate through the facility. It can be seen that unstart limits the increase in test time for PALM to a factor of 10.

The total temperature in each mode is shown in Fig 5a. All traces exhibit a transient increase in total temperature at the start of the test as a result of the unsteady filling of the nozzle plenum. Ludwieg mode fills the plenum fastest, and consequently the magnitude of the transient increase is greatest. However, the steady state total temperature is consistent within the +/-15 K uncertainty of the aspirated thermocouples across all modes.

Fig 5b shows a comparison between the unit Reynolds number, calculated using Keyes' relation for viscosity and assuming isentropic expansion through the facility nozzle. Again, this follows the supply pressure trace. Due to the reduction in supply pressure, operation in PALM has enabled testing at lower unit Reynolds numbers than HDT would typically be able to reliably produce in Ludwieg Mode.

Finally, Table 1 presents a summary of the test duration and steadiness across the modes of operation. All values for Ludwieg Mode have been averaged on the second plateau. It can be seen that PALM offers a factor of 10 increase in test time relative to LM, but exhibits a shorter test duration than ELM due to the longer facility startup shown in Fig. 4a. Additionally, PALM offers a significant improvement in the steadiness of the test time relative to both ELM and LM at Mach 7.

V. Performance Map

This section presents the potential performance of the HDT operating in PALM in terms of unit Reynolds number and test time achievable based on numerical simulations. It begins with the theoretical maximum, before discussing practical limitations and their effects on the resultant performance. The section concludes with some recommendations for future upgrades to HDT to achieve the maximum test time.

Numerical simulations of HDT operating in the PALM were performed in L1D [20, 21], a quasi-one dimensional Lagrangian flow solver used extensively in the design of hypersonic facilities [22–24]. A description of the L1D geometry, along with the tuning against LM data (achieved by the addition of head loss and heat transfer augmentation patches), is given in [17]. Fig. 6 shows a comparison of these simulations against the presented PALM data. The numerical traces are performed with a more ideal valve opening and consequently exhibit a faster rise time than experimental data, as well as a slightly steadier plateau. However, it can be seen that HDT's performance in PALM is well predicted by the L1D simulations.

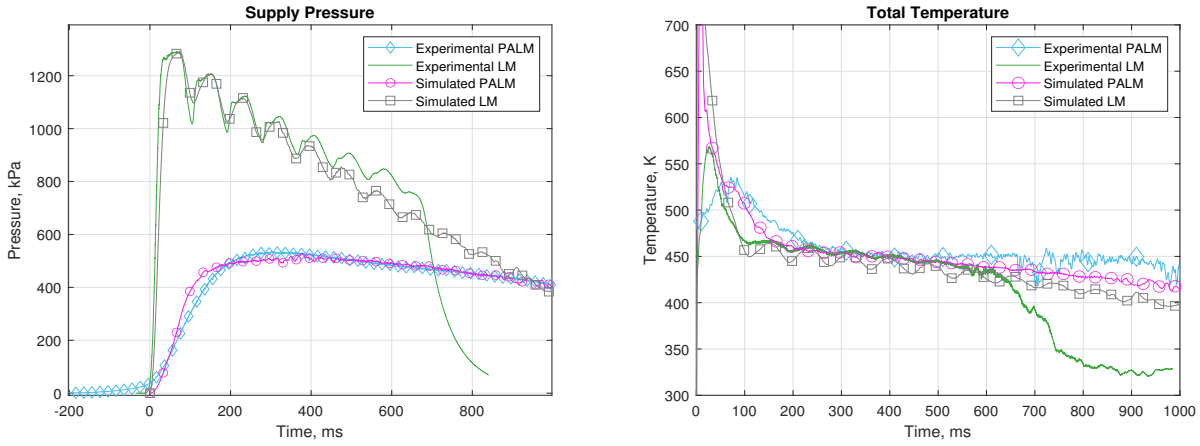

(a) Supply Pressure

(b) Total Temperature

Fig. 6 Comparison between experimental and simulated PALM traces in HDT at Mach 7, 14 bar, 500 K fill, with $x_{wr} = 0.4x_1$.

A. Theoretical

To characterise the theoretical performance of HDT operating in PALM, L1D simulations were performed at the maximum rated fill pressure (275 bar) of the facility. Fig 7 shows transient supply pressure and unit Reynolds number for two cases, one with $x_{wr} = 0.6x_1$ and the other $x_{wr} = 0.3x_1$, to illustrate a range of PALM capability. The value of x_{wr} chosen for the simulations is somewhat arbitrary but is expected to bound physically realisable values. It can be seen that $x_{wr} = 0.3x_1$ offers a supply pressure of approximately 75 bar and Unit Reynolds number of 40×10^6 m^{-1} for a test time approaching 1 second. Noting that the maximum unit Reynolds number achieved in HDT to date is 33×10^6 m^{-1}, this presents a significant expansion of the test time capability for the range of Unit Reynolds numbers over which HDT has previously operated. However, higher unit Reynolds numbers can still be achieved, with the $x_{wr} = 0.6x_1$ case offering Unit Reynolds numbers of 90×10^6 m^{-1} at a reduced test time of 300 ms.

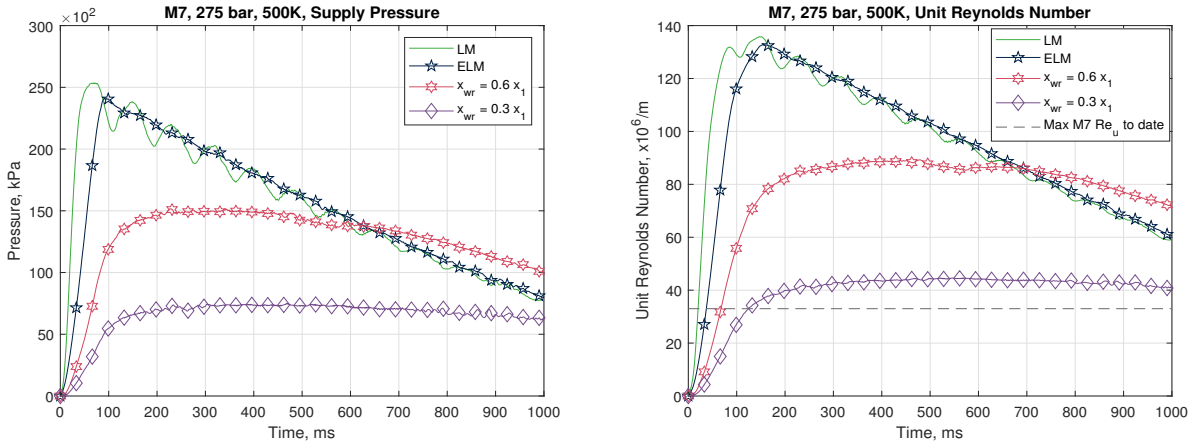

(a) Supply Pressure

(b) Unit Reynolds Number

Fig. 7 L1D simulations of LM, ELM and PALM in HDT at Mach 7, 275 bar, 500 K

B. Practical Limitations

1. Fill Pressure

The first practical limitation considered on is the maximum fill pressure able to be run without risking damage to the facility. The HDT test section and dump tank have a pressure rating of 1 bar absolute. Consequently, in order to avoid test section over-pressurisation, the fill pressure of HDT is limited to 100 bar at Mach 7, significantly reducing the unit Reynolds number capability.

2. Facility Unstart

As shown in Fig. 4b, the test flow in HDT unstarts before the test is terminated. To investigate the cause of this unstart and to characterise how this limits HDT's maximum test time, the output of L1D simulations were used in an unsteady filling calculation to predict the transient pressure inside the test section and dump tank. The inputs to the calculator are nozzle supply pressure and total temperature. At each timestep, the pressure ratio between volumes is calculated to determine whether the flow between them is choked and then the appropriate mass flow is calculated (choked or subsonic). The calculator was validated with experimental supply pressure, total temperature and Pitot pressure data from a 50 bar, 500 K LM experiment. Fig 8a shows the predicted test section and dump tank pressures, with experimental centreline Pitot pressure overlaid. The test section pressure exhibits a distinct change in form at $t = 520$ ms due to the pressure ratio between the test section and dump tank reducing below the choked flow limit, which corresponds well with the unstart observed at $t = 535$ ms in the experimental Pitot trace. It is likely that the premature unstart is therefore a result of the flow between test section and dump tank becoming unchoked, allowing pressure waves to travel upstream from the dump tank and terminate the test.

Fig. 8b shows a comparison between predicted test section pressure in LM and PALM for a 100 bar fill condition. It

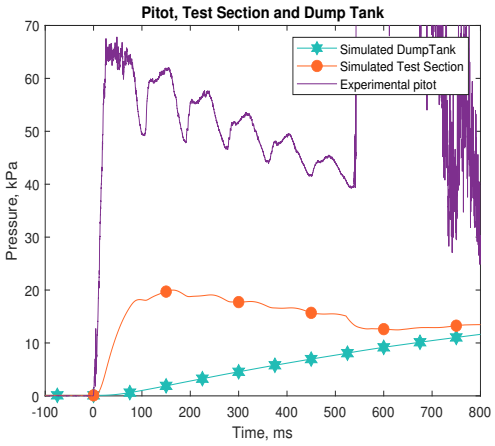

(a) Experimental validation

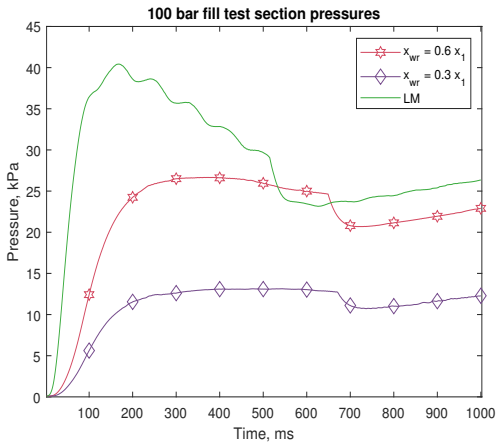

(b) 100 bar fill

Fig. 8 Output of the unsteady filling calculator used to estimate effect of unstart

can be seen that LM is predicted to unstart at $t = 515$ ms, PALM at $t = 650$ ms and $t = 670$ ms for $x_{wr} = 0.6x_1$ and $x_{wr} = 0.3x_1$, respectively. The delay in unstart with lower values of x_{wr} is expected due to the reduced mass flow. This predicts that the actual test time for the $x_{wr} = 0.6x_1$ case is unaffected by unstart, as this occurs at approximately the same time as the plateau ends. Consequently, it can be seen that unstart currently only impedes the test time for values $x_{wr} < 0.6x_1$.

C. Current Performance

Fig 9a shows the output of M7 L1D simulations with a 100 bar, 500 K fill condition. More simulations have been performed at this fill condition with different values of x_{wr} to fully demonstrate the predicted performance capability with an ideally operating plug valve. Fig 9b illustrates the current performance of the HDT operating in PALM. It can be seen that the current test time is limited to approximately 400 ms, with unit Reynolds numbers of approximately 32×10^6 m^{-1} possible. Noting the maximum M7 unit Reynolds number run in the HDT to date is approximately 33×10^6 m^{-1}, PALM presents a factor of 10 improvement in test time for all Mach 7 unit Reynolds numbers run to date in the facility.

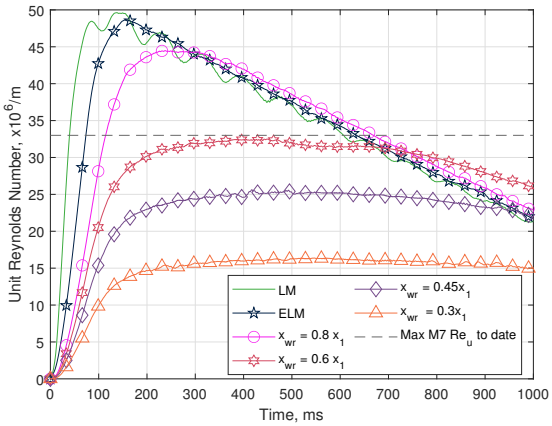

(a) Unit Reynolds Number with 100 bar, 500 K fill

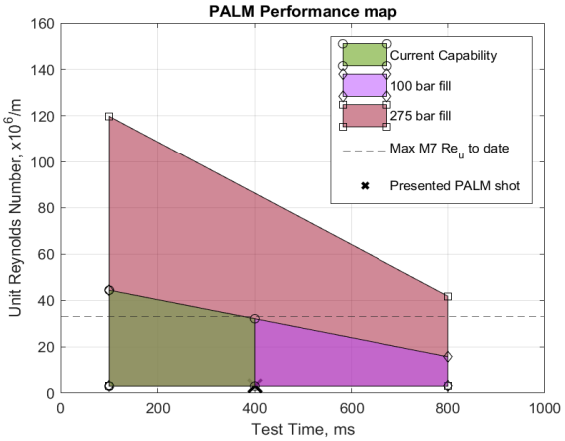

(b) Performance map

Fig. 9 Performance capability of the HDT operating in PALM at Mach 7.

D. Potential Facility Upgrades

There are three key recommendations for facility upgrades in order to maximise HDT's test time performance:

- Pressure test facility test section, dump tank and other downstream infrastructure to a minimum of 5 bar absolute.
- Redesign ducting between test section and dump tank to form a supersonic diffuser.
- Increase dump tank volume

The first upgrade will increase the unit Reynolds number capability, whilst the latter two will increase the achievable test time (before unstart). The authors note that whilst the presented analysis was conducted at Mach 7, the recommended upgrades maximise performance across all of the current HDT nozzles.

VI. Conclusion

This paper has presented experimental results for the Oxford High Density Tunnel operating in Plenum Augmented Ludwieg Mode (PALM), a mode of operation designed to extend the test time in Ludwieg Tunnels. A theoretical performance map for the HDT operating in PALM has been presented, and recommendations made to enhance HDT's current test time performance. It is worth noting that due to the increased duration of facility startup, PALM is currently unsuitable for certain experiments (e.g. free-flight force measurements [25]). Additionally, increased test time may be detrimental for heat transfer experiments, as the 1D semi-infinite wall assumption often used in the data reduction may no longer be valid. However, operation in PALM has been experimentally demonstrated to offer a factor of 10 improvement in test time with an approximately 50% reduction in Unit Reynolds number capability relative to standard Ludwieg Mode. Theoretical performance maps predicts that PALM can offer a factor of 10 improvement in test time for all Mach 7 unit Reynolds numbers run to date in the facility without any facility upgrades. This improvement in test time significantly expands the capability of the HDT for investigating both steady and unsteady phenomena, for example force balance measurements, fluid-structure interaction, high speed inlet characterisation, and wake flows. Prior to development of PALM, an order of magnitude increase in steady test time in Ludwieg Tunnels would only have been possible with an order of magnitude increase in facility length. Hence, if any operator of a Ludwieg Tunnel desires to increase facility test time, the authors recommend retrofitting a plenum between the barrel and nozzle and implementing PALM.

Acknowledgments

This research was funded and supported by DSTL. The authors would also like to thank Hal Surtell and William Godfrey for installing the PALM pipework, and Tristan Crumpton and Harry Kachika for operation of HDT in the new modes.

References

[1] Schneider, S. P., "Flight data for boundary-layer transition at hypersonic and supersonic speeds," *Journal of Spacecraft and Rockets*, Vol. 36, No. 1, 1999, pp. 8–20.

[2] Ferlemann, S., McClinton, C., Rock, K., and Voland, R., "Hyper-X Mach 7 scramjet design, ground test and flight results," *AIAA/CIRA 13th International Space Planes and Hypersonics Systems and Technologies Conference*, 2005, p. 3322.

[3] Wadhams, T., MacLean, M., Holden, M., and Barry, S., "A review of transition studies on full-scale flight vehicles at duplicated flight conditions in the LENS tunnels and comparisons with prediction methods and flight measurement," *48th AIAA Aerospace Sciences Meeting Including the New Horizons Forum and Aerospace Exposition*, 2010, p. 1246.

[4] Cockre, C., Auslender, A., White, J., and Dilley, A., "Aeroheating predictions for the X-43 hyper-X cowl-closed configuration at Mach 7 and 10," *40th AIAA Aerospace Sciences Meeting & Exhibit*, 2002, p. 218.

[5] Gu, S., and Olivier, H., "Capabilities and limitations of existing hypersonic facilities," *Progress in Aerospace Sciences*, Vol. 113, 2020, p. 100607.

[6] Lu, F. K., and Marren, D. E., "Principles of hypersonic test facility development," *Progress in Astronautics and Aeronautics. Volume 198*, 2002, pp. 17–27.

[7] Stalker, R., "Modern developments in hypersonic wind tunnels," *The Aeronautical Journal*, Vol. 110, No. 1103, 2006, pp. 21–39.

[8] Davies, W., and Bernstein, L., "Heat transfer and transition to turbulence in the shock-induced boundary layer on a semi-infinite flat plate," *Journal of Fluid Mechanics*, Vol. 36, No. 1, 1969, pp. 87–112.

[9] East, R., Stalker, R., and Baird, J., "Measurements of heat transfer to a flat plate in a dissociated high-enthalpy laminar air flow," *Journal of Fluid Mechanics*, Vol. 97, No. 4, 1980, pp. 673–699.

[10] Jacobs, P., Rogers, R., Weidner, E., and Bittner, R., "Flow establishment in a generic scramjet combustor," *Journal of Propulsion and Power*, Vol. 8, No. 4, 1992, pp. 890–899.

[11] Sanderson, S., and Simmons, J., "Drag balance for hypervelocity impulse facilities," *AIAA journal*, Vol. 29, No. 12, 1991, pp. 2185–2191.

[12] Mee, D. J., "Dynamic calibration of force balances for impulse hypersonic facilities," *Shock Waves*, Vol. 12, 2003, pp. 443–455.

[13] Doherty, L. J., Smart, M. K., and Mee, D., "Measurement of three-components of force on an airframe integrated scramjet at Mach 10," *20th AIAA International Space Planes and Hypersonic Systems and Technologies Conference*, 2015, p. 3523.

[14] Wylie, S., Doherty, L., and McGilvray, M., "Commissioning of the Oxford high density tunnel (HDT) for boundary layer instability measurements at Mach 7," *2018 Fluid Dynamics Conference*, 2018, p. 3074.

[15] Dufrene, A. T., "Extension of LENS shock tunnel test times and lower Mach number capability," *53rd AIAA Aerospace Sciences Meeting*, 2015, p. 2017.

[16] Jones, T., Street, P., and Westby, M., "Recent enhancements to the DRA shock tunnel," *Wind tunnels and wind tunnel test techniques*, 1992, p. 30.

[17] Hillyer, J., Doherty, L., Hambidge, C., and McGilvray, M., "Extension of test time in Ludwieg Tunnels," 2022.

[18] McGilvray, M., Doherty, L. J., Neely, A. J., Pearce, R., and Ireland, P., "The oxford high density tunnel," *20th AIAA International Space Planes and Hypersonic Systems and Technologies Conference*, 2015, p. 3548.

[19] Herman T., M. M. H. C., and Buttsworth D., "Total Temperature Measurements In the Oxford High Density Tunnel," *FAR Conference, Monopoli, Italy*, 2019.

[20] Jacobs, P., "Quasi-one-dimensional modeling of a free-piston shock tunnel," *AIAA journal*, Vol. 32, No. 1, 1994, pp. 137–145.

[21] Jacobs, P. A., "Shock tube modelling with L1d," 1998.

[22] Collen, P., Doherty, L. J., Subiah, S. D., Sopek, T., Jahn, I., Gildfind, D., Penty Geraets, R., Gollan, R., Hambidge, C., Morgan, R., et al., "Development and commissioning of the T6 Stalker Tunnel," *Experiments in Fluids*, Vol. 62, No. 11, 2021, pp. 1–24.

[23] Andrianatos, A., "Ground Testing at Superorbital Flight Conditions in a Large Scale Expansion Tube," 2020.

[24] Mundt, C., Selcan, C., and Sander, T., "Investigations in the piston driven shock-tunnel HELM," 2019.

[25] Hyslop, A. M., McGilvray, M., and Doherty, L. J., "Free-Flight Aerodynamic Testing of a 7 Degree Half-Angle Cone," *AIAA SCITECH 2022 Forum*, 2022, p. 1324.